Published in final edited form as:
Cancer Res. 2014 December 1; 74(23): 6784–6795. doi:10.1158/0008-5472.CAN-14-0043.

MHC-restricted phosphopeptides derived from Insulin receptor substrate-2 and CDC25b offer broad-based immunotherapeutic agents for cancer

Angela L. Zarling[1], **Rebecca C. Obeng**[1], **A. Nicole Desch**[1], **Joel Pinczewski**[2,3], **Kara L. Cummings**[1], **Donna H. Deacon**[3,4], **Mark Conaway**[5], **Craig L. Slingluff Jr.**[3,4], and **Victor H. Engelhard**[1]

[1]Carter Immunology Center and Department of Microbiology, Immunology and Cancer Biology, University of Virginia, Charlottesville, VA 22908

[2]Department of Pathology, University of Virginia, Charlottesville, VA 22908

[3]Human Immune Therapy Center, University of Virginia, Charlottesville, VA 22908

[4]Department of Surgery, University of Virginia, Charlottesville, VA 22908

[5]Department of Public Health Sciences, University of Virginia, Charlottesville, VA 22908

Abstract

Cancer cells display novel phosphopeptides in association with MHC class I and II molecules. In this study, we evaluated two HLA-A2-restricted phosphopeptides derived from the insulin receptor substrate (IRS)-2 and the cell cycle regulator CDC25b. These proteins are both broadly expressed in multiple malignancies and linked to cancer cell survival. Two phosphopeptides, termed pIRS-$2_{1097\text{-}1105}$ and pCDC25$b_{38\text{-}46}$, served as targets of strong and specific CD8 T-cell memory responses in normal human donors. We cloned T-cell receptor (TCR) cDNAs from murine CD8 T-cell lines specific for either pIRS-$2_{1097\text{-}1105}$ or pCDC25$b_{38\text{-}46}$. Expression of these TCR in human CD8 T-cells imparted high-avidity phosphopeptide-specific recognition and cytotoxic and cytokine-secreting effector activities. Using these cells, we found that endogenously processed pIRS-$2_{1097\text{-}1105}$ was presented on HLA-$A2^+$ melanomas and breast, ovarian, and colorectal carcinomas. Presentation was correlated with the level of the Ser^{1100}-phosphorylated IRS-2 protein in metastatic melanoma tissues. The highest expression of this protein was evident on dividing malignant cells. Presentation of endogenously processed pCDC25$b_{38\text{-}46}$ was narrower, but still evident on HLA-$A2^+$ melanoma, breast carcinoma and lymphoblastoid cells. Notably, pIRS-$2_{1097\text{-}1105}$-specific and pCDC25$b_{38\text{-}46}$-specific TCR-expressing human CD8 T-cells markedly slowed tumor outgrowth *in vivo*. Our results define two new antigens that may be developed as immunotherapeutic agents for a broad range of HLA-$A2^+$ cancers.

Corresponding author: Victor H. Engelhard, Carter Immunology Center, University of Virginia, Box 801386, 345 Crispell Drive, Charlottesville, VA 22908-1386 USA. vhe@virginia.edu (434) 924-2423; (434) 924-1221 fax.

Conflict of Interest: ALZ, RCO, KLC, and VHE acknowledge conflicting financial interests as shareholders in PhosImmune, Inc.

Keywords

CD8 T-cells; cancer antigen; protein phosphorylation

Introduction

Clinical trials using adoptive cellular therapy and vaccination have demonstrated the importance of CD8 T-cells in controlling cancer (1–4). A large number of tumor-associated antigens (TAA) recognized by CD8 T-cells have been identified in the last 20 years, and clinical tumor regressions have been associated with immunotherapies based on some of them (1,5). However, clinical response rates to vaccines targeting a range of TAA have been disappointing (6). The repertoire of TAA include: i) neo-antigens formed by mutations in cellular proteins; ii) antigens induced by oncogenic viruses; iii) cancer-testis antigens normally expressed only in germ-line cells; and iv) tissue-specific differentiation antigens (7). Only a small number of TAA source proteins have been linked to either initial cellular transformation processes or later tumorigenic processes such as angiogenesis and metastasis (8,9). Targeting TAA derived from proteins that are vital for a cancer cell's survival and metastatic potential is attractive, since down-regulation and/or mutation of genes encoding these proteins as a means of immune evasion could compromise cellular malignancy (10,11).

Many signaling pathways that involve protein phosphorylation and dephosphorylation are altered in cancer cells, and some of these have been directly associated with alterations in cellular growth, survival, and metastasis (12,13). We hypothesized that proteolytic processing of malignancy-associated phosphorylated proteins would yield a pool of phosphopeptides that could be presented by MHC-I and MHC-II molecules on tumor cells, and serve as targets of anti-tumor adaptive immunity. We have demonstrated that phosphopeptides are presented by many different MHC-I and MHC-II molecules (14–17), and that many phosphopeptides presented by HLA-A2 on melanoma and ovarian cancer cell lines (16), and by HLA-B7 on leukemic malignancies (17) were derived from source proteins that are either over-expressed or dysregulated in cancer cells. We were particularly interested in HLA-A2-restricted phosphopeptides derived from insulin receptor substrate (IRS)-2 and cell division cycle 25b (CDC25b): pIRS-$2_{1097\text{-}1105}$ and pCDC25$b_{38\text{-}46}$.

IRS proteins are adapters that link signaling from growth factor and cytokine receptors, including the insulin receptor, insulin-like growth factor receptor and IL-4 receptor, to multiple SH2-containing signaling proteins to modulate cellular growth, metabolism, survival and differentiation (18). IRS-2 is over-expressed at the gene or protein level in pancreatic cancer (19), hepatocellular carcinoma (20), neuroblastoma (21), breast cancer (22), glioblastoma (23), and colorectal cancer (24). IRS-2 over-expression under a mouse mammary tumor virus promoter causes mammary hyperplasia, tumorigenesis and metastasis (22,25–27). The IRS proteins are regulated by phosphorylation of Tyr, Ser and Thr (18). Phosphorylation of Ser^{1100} in IRS-2 (pSer^{1100}-IRS-2) was unknown until identification of the pIRS-$2_{1097\text{-}1105}$ phosphopeptide by mass spectrometry (16). Little is known about the function of this site, although it is highly phosphorylated in M phase (28). However, the

breadth of expression of pIRS-$2_{1097\text{-}1105}$ among different cancer cells has not been investigated. CDC25 dual-specificity phosphatases regulate the activity of cyclin-dependent kinases by dephosphorylation of Tyr and Thr residues in their active sites (29). CDC25b is a target of p38, and regulates the activity of the cyclin B1/CDK1 complex, which promotes the G_2-M transition (30). CDC25b over-expression in multiple malignancies is correlated with poor prognosis (29). However, as with IRS-2, phosphorylation of CDC25b at Ser^{42} has not been previously described and the immunological display of the HLA-A2 restricted pCDC25$b_{38\text{-}46}$ phosphopeptide on different cancer cells has not been evaluated.

Our main goal in this study was to evaluate the breadth of expression of pIRS-$2_{1097\text{-}1105}$ or pCDC25$b_{38\text{-}46}$ phosphopeptides on cancers and to evaluate their immunotherapeutic potential.

Materials and Methods

Cell line care

Breast cancer cell lines were maintained in complete DMEM medium (containing 10% FBS, 2 mM L-glutamine, 15mM Hepes, and Pen/Strep). Melanoma, ovarian carcinoma, and colo-rectal cancer lines were maintained in complete RPMI-1640 (16). Transfectants of the B lymphoblastoid cell line C1R expressing either HLA-A2 (C1R-A2) or a chimeric HLA-A2/D^d MHC-I molecule (C1R-AAD) were maintained in complete RPMI with 300 μg/ml Hygromycin B or G418 (Cellgro), respectively (16).

Human CD8 T-cell culture and IFN-γ ELISpot

Magnetic bead-enriched (Miltenyi; 130-096-495) human CD8 T-cells were co-cultured with irradiated, peptide-pulsed matured DC for 7d in individual 96-well microcultures at a 15:1 ratio (31). In some experiments, enriched CD8 T-cells were further magnetic bead-enriched for $CD45RO^+$ cells (Miltenyi; 130-046-001). An indirect ELISpot was performed as described (32) using 25,000 cells/well with or without 75,000 peptide-pulsed (10 μg/ml) T2 targets. All human protocols were approved by the UVA IRB for Health Sciences Research.

Generation of murine phosphopeptide-specific T-cells

Murine CD8 T-cells specific for pIRS-$2_{1097\text{-}1105}$ (RVA[pS]PTSGV) or pCDC25$b_{38\text{-}46}$ (GLLG[pS]PVRA) were generated in AAD transgenic mice as described (14,16). pβ-catenin$_{30\text{-}39}$ (YLD[pS]GIHSGA), Yellow Fever NS4$B_{214\text{-}222}$ (LLWNGPMAV), and $M1_{58\text{-}66}$ Flu (GILGFVFTL) peptides were used as controls. Peptides were synthesized by GenScript or Biosynthesis Inc. All protocols were approved by the UVA Institutional Animal Care and Use Committee.

Cloning of phosphopeptide-specific murine TCR α and β chains

pIRS-$2_{1097\text{-}1105}$-specific or pCDC25$b_{38\text{-}46}$-specific murine T-cell lines were magnetically enriched for CD8α (Miltenyi, 130-049-401). Total RNA was isolated using PureLink Micro-to-Midi Total RNA isolation kit (Invitrogen) and cDNA was synthesized using the GeneRacer™ Kit (Life Technologies) as described (33). 5′RACE PCR was performed using the GeneRacer™ 5′ primer and one of three 3′ gene-specific primers: TCR-CαRev (5′-

ACTGGACCACAGCCTCAGCGTCAT-3′), TCR-Cβ1Rev (5′-TGAATTCTTTCTTTTGACCATAGCCAT-3′) or TCR-Cβ2Rev (5′GGAATTTTTTTTCTTGACCATGGCCAT-3′). PCR products of correct size were cloned into the pCR®4-TOPO® vector (Life Technologies). TCR sequences were determined and matched to the IMGT database (34). TCR sequences are found under GenBank accession nos. KJ542620, KJ542621, KJ542622 and KJ542623.

Electroporation of in vitro transcribed (IVT) RNA encoding phosphopeptide-specific TCR chains

IVT RNA of TCR αβ chains and transfection of OKT3-activated human CD8 T-cells was performed as described (35,36). The 5′ primers included sequence for T7 RNA polymerase binding and transcription, followed by a Kozak sequence, a start codon and the next 16–17 bp of Vα or Vβ region for each TCR gene while the 3′ primers included 66 T residues and 16–25 bp of the relevant α or β constant region sequence. pIRS-$2_{1097\text{-}1105}$-specific TCRα cDNA was amplified using the 5′ primer (5′-TAATACGACTCACTATAGGGAGAGCCACCATGCTCCTGGCACTCCTCCC-3′) and pIRS-$2_{1097\text{-}1105}$-specific 3′ primer (5′-T_{66}AACTGGACCACAGCCTCAGCGTC-3′) while the TCRβ was amplified using 5′primer (5′-TAATACGACTCACTATAGGGAGAGCCACCATGGGCACCAGGCTTCTTGG-3′) and the 3′primer (5′-T_{66}AGGAATTTTTTTTCTTGACCATGGCC-3′). pCDC25$b_{38\text{-}46}$-specific TCRα cDNA was amplified using the 5′ primer: (5′-TAATACGACTCACTATAGGGAGAGCCACCATGAAGACAGTGACTGGACC-3′) and the pIRS-2 3′ reverse primer, while the pCDC25b TCRβ was amplified using 5′primer (5′-TAATACGACTCACTATAGGGAGAGCCACCATGTCTAACACTGCCTTCCCT-3′) and the pIRS-2 TCRβ 3′ primer.

T-cells were transfected using the BTX T820 electroporation system and BTX 2mm gap cuvettes. Cells (5×10^6) in 0.2 ml serum-free OPTI-MEM (Life Technologies) were mixed with 10 μg IVT RNA of each TCR α and β chain and pulsed at 500V for 0.3msec. Transfected cells were placed in AIM-V (Life Technologies) with 5% AB^+ serum (Gemcell).

Functional analysis of phosphopeptide-specific murine TCR-expressing human CD8 T-cells

Fourteen-16 hours post-electroporation, human CD8 T-cells were co-cultured with peptide-pulsed or unpulsed C1R-AAD, C1R-A2 or cancer cells endogenously expressing pIRS-$2_{1097\text{-}1105}$ or pCDC25$b_{38\text{-}46}$. Cell surface expression of mouse TCRβ, and human CD3 and CD8 was assessed using antibodies from Becton Dickinson Bioscience or eBioScience. During a 5h co-culture of stimulator cells with TCR-transfected CD8-T cells at 37°C, anti-human CD107a-Alexa 647 (eBioScience) was added in the presence of 5 μg/ml Brefeldin A (Sigma), 5 μg/ml Monensin (eBioscience) and 300 IU/ml human IL-2 (Chiron or R & D Systems). Cells were then stained for surface molecules, fixed and permeabilized using Cytofix/Cytoperm (BD) and stained for intracellular cytokine (anti-IFN-γ and anti-TNF-α, eBioscience). Immunofluoresence was analyzed using Becton Dickinson FACS Canto I or Canto II flow cytometers and FlowJo software.

In Vitro cytotoxicity assay

Phosphopeptide-specific TCR-expressing CD8 T-cells were co-cultured for 5h with a 1:1 mix of C1R-A2 cells pulsed with 1μM phosphopeptide and stained with 1 μM carboxyfluorescein succinimidyl ester (CFSE; Life Technologies) and unpulsed C1R-A2 cells stained with 0.1 μM CFSE. Specific killing was assessed by evaluating percent loss of the peptide-pulsed population relative to the unpulsed population.

Western analysis

Lysates were generated as described (16) or using NE-PER protein extraction kit (Thermo Fisher) and separated on 8–16% gradient SDS/PAGE gels (ISC BioExpress or Thermo Scientific). Proteins were transferred to Immobilon FL PVDF (Millipore) membranes, which were blocked and probed with pSer^{1100}-IRS-specific and GAPDH-specific Ab (Santa Cruz, SC-25778) as described (16). Blots were then stripped with Restore Plus (Thermo Scientific) and reprobed with anti-IRS-2 (Santa Cruz, H-205). Total CDC25b protein was detected with anti-CDC25b (C-20, Santa Cruz). A HEK293T line transfected to express CDC25b (Novus Biological) was used as a positive control for anti-CDC25b. Pixel densities were determined using AlphaEase FC software.

Immunohistochemistry

Formalin-fixed paraffin-embedded cell line pellets and tissue microarrays of metastatic melanoma (UVA Biorepository and Tissue Research Facility) were deparaffinized, rehydrated, counterstained with hematoxylin, incubated with anti-Ser^{1100}-pIRS-2 (16) for 3h at 4°C after antigen retrieval, and specific antibody staining was detected using AEC ImmPACT (Vector Labs). Antibodies were removed with ethanol and acidified potassium permanganate and then reprobed with anti-IRS-2 (Santa Cruz). Total intensities and areas of representative fields stained with anti-Ser^{1100}-pIRS-2 (16) in the absence or presence of blocking peptide were evaluated using the “Positive Pixel Count” algorithm on an Aperio Scanner, which accounts for the number of pixels with significant staining and staining intensity of each pixel. Staining densities (total intensity/mm^2) were calculated for representative sections in the absence of blocking peptide, and subtracted from staining densities of representative sections from peptide-blocked slides to determine specific staining densities of each metastatic melanoma and adjacent uninvolved tissues.

Tumor control

Seven to 8wk old male NOD/SCID/IL-2Rγc$^{-/-}$ (Jackson Immunoresearch) mice were inoculated subcutaneously with 1.4 × 10^6 AAD$^+$ SLM2 melanoma cells. Three x10^6 human CD8 T-cells expressing either pIRS-2- or pCDC25b-specific TCR, or 1.5×10^6 of both populations, were adoptively transferred 3d later. An additional 1.5 × 10^6 T-cells were given 4d later. All mice received 1500 CU of IL-2 (R & D Systems) i.p. every other day for 10d. Tumor size was measured every 2–3d with a digital caliper, and calculated as LxW (mm^2). Animals were considered tumor free until the evaluation day when the tumor size was measurable (>30 mm^2). Non-transfected human CD8 T-cells from both donors utilized did not recognize SLM2 melanoma *in vitro* (data not shown).

Statistical analysis

Tests performed to determine statistical significance are indicated in the figure legends. P values less than 0.05 were considered significant.

Results

Immunogenicity of phosphopeptides for human donors in vitro

The pIRS-$2_{1097\text{-}1105}$ and pCDC25$b_{38\text{-}46}$ phosphopeptides were initially identified on two melanomas and an ovarian carcinoma (16), but their ability to induce T-cell responses in humans was not evaluated. Thus, we cultured T-cells from normal human donors in replicate microwells with autologous mature dendritic cells (DC) pulsed with either phosphopeptide. After 7 days, T-cells in these cultures produced IFN-γ when restimulated with phosphopeptide-pulsed HLA-$A2^+$ targets (Figure 1A, B). They did not recognize targets pulsed with the unphosphorylated homologous peptide (Figure 1B). The magnitude of these responses was surprisingly high. Donor 44's phosphopeptide-specific responses were significantly greater than that to a yellow fever virus peptide (LLWNGPMAV), to which this donor had not been previously exposed. Donor 54 had been immunized with yellow fever vaccine and this individual's phosphopeptide specific responses were somewhat lower than the yellow fever response although still strong (Figure 1A). We recently established that immunity to some leukemia-associated phosphopeptides in normal individuals resides in the central memory compartment, suggesting prior exposure in conjunction with immune surveillance (17). Thus, we isolated $CD45RO^+$ memory CD8 T-cells from 4 different donors and stimulated them with autologous DC pulsed with either pIRS-$2_{1097\text{-}1105}$ or pCDC25$b_{38\text{-}46}$ for 7 days. Using a cutoff of >50 spots/25,000 cells, all 4 donors showed moderate to strong pre-existing memory responses to the pCDC25$b_{38\text{-}46}$ peptide, and 2/4 donors responded to pIRS$2_{1097\text{-}1105}$ (Figure 1C). In all cases, the T-cells were specific to the phosphorylated peptide and did not recognize the unphosphorylated homolog (not shown). The magnitude of these memory responses was quite variable among peptides and donors, but was in some cases equivalent to or greater than memory responses to influenza and/or yellow fever epitopes (Note: donors 54 and 62 had been immunized with a yellow fever vaccine. Donors 43 and 44 are yellow fever naïve). This is inconsistent with the development of self-tolerance to these phosphopeptides. Combined, the strength of the responses in Figure 1 is consistent with the possibility that these four normal human donors have been previously exposed to both phosphopeptides. However, none of these donors have indications of autoimmune disease, consistent with the possibility that these phosphopeptides are not displayed on normal tissue.

Functional activity of phosphopeptide-specific murine TCR upon expression in human CD8 T-cells

Adoptive transfer of human T-cells transfected with cloned high affinity tumor-reactive TCR can lead to positive clinical responses in cancer patients (2,37–39). These TCR also enable the expression of endogenously processed and presented TAA on cancers of multiple types to be determined. In addition to the constraints of growing human T-cells *in vitro* (40), tolerance mechanisms are believed to purge most of the high affinity CD8 T-cells that would mediate effective tumor regression (39). A method to isolate human TAA-specific T-cells

with TCRs of sufficient functional avidity to mediate tumor regression is through the immunization of HLA transgenic mice (39,41). Murine TCRs are of similar structural homology to human TCRs such that they can be incorporated into the human CD3 complex and preferentially pair upon expression in human T-cells (37,41). We previously demonstrated that these phosphopeptides were immunogenic following *in vivo* immunization of HLA-A2 transgenic mice (16). To avoid the generation of unintended cross-reactivities through pairing of transfected and endogenous human TCR chains, we utilized HLA transgenic mice to elicit phosphopeptide-specific murine T-cells, from which TCR cDNAs were cloned. AAD mice, expressing a class I MHC molecule that contains the α1 and α2 domains from HLA-A2, and the α3, transmembrane, and cytoplasmic domains from H-2D^{d}, were immunized with autologous DC pulsed with either pIRS-2$_{1097\text{-}1105}$ or pCDC25b$_{38\text{-}46}$. CD8 T-cell lines derived from these animals secreted IFN-γ when cultured with AAD^{+} targets pulsed with the phosphorylated forms of these epitopes but not their non-phosphorylated counterparts (Figure 1D). However, they failed to recognize phosphopeptide-pulsed targets expressing fully human HLA-A2, most likely due to the low affinity of murine CD8 for the human α3 domain (37,42). cDNAs encoding the TCR α and β chains from pIRS-2$_{1097\text{-}1105}$–specific (Supplemental Figure 1) or pCDC25b$_{38\text{-}46}$–specific (Supplemental Figure 2) T-cell lines were molecularly cloned and utilized as templates to produce *in vitro* transcribed (IVT) RNA (33,36). Electroporation of IVT RNA into either TCR-deficient SupT1 cells or human CD8 and CD4 T-cells resulted in surface expression as detected by staining for mouse TCRβ (Supplemental Figure 3A, 3B). TCR expression was detected at high levels at 9h (Supplemental Figure 3B) with some TCR still detectable 5d post-electroporation (Supplemental Figure 3C).

Human CD8 T-cells electroporated with IVT RNA encoding either TCR produced IFN-γ and/or upregulated CD107a, a marker of cytotoxic activity, in a dose-dependent manner after co-culture with phosphopeptide-pulsed AAD^{+} targets (Figure 2A, 2B). Both TCR conferred half-maximal recognition at a peptide dose of ~400–800 pM. In contrast to the murine T-cells expressing these TCR (Figure 1D), the human CD8 T-cells recognized phosphopeptide-pulsed targets expressing HLA-A2 at least as well as those expressing AAD (Figure 2A, 2B). Neither cell produced IFN-γ or upregulated CD107a in response to HLA-A2^{+} targets pulsed with high levels of the non-phosphorylated peptide. Human CD8 T-cells expressing the pIRS-2-specific murine TCR also killed pIRS-2$_{1097\text{-}1105}$-pulsed, but not pCDC25b$_{38\text{-}46}$-pulsed, targets *in vitro* (Figure 2A), while those expressing the pCDC25b-specific TCR killed pCDC25b$_{38\text{-}46}$-pulsed but not pIRS-2$_{1097\text{-}1105}$ or pβ-catenin$_{30\text{-}39}$-pulsed targets (Figure 2B). Thus, the expression of these murine TCR in human CD8 T-cells imparts phosphopeptide-specific, high-avidity recognition and both cytotoxic and cytokine-secreting effector activities.

Expression of pIRS-2$_{1097\text{-}1105}$ and pCDC25b$_{38\text{-}46}$ phosphopeptides on cancer cells

We next evaluated whether these transfected CD8 T-cells could recognize endogenously processed and presented pIRS-2$_{1097\text{-}1105}$ or pCDC25b$_{38\text{-}46}$ phosphopeptide on HLA-A2^{+} cancer cell lines. To correlate pIRS-2$_{1097\text{-}1105}$-specific T-cell recognition with phosphoprotein expression, we used an antibody specific for the Ser^{1100}-phosphorylated IRS-2 protein (pSer^{1100}-IRS-2) as well as an antibody that recognizes total IRS-2 protein

(16). A substantial fraction of pIRS-$2_{1097\text{-}1105}$-specific T-cells upregulated CD107a, and a subset of these also produced IFN-γ, upon co-culture with two HLA-$A2^+$ melanoma cell lines, MelSwift and 1102Mel (Figure 2C). These two cell lines also expressed high levels of $pSer^{1100}$-IRS-2 (Figure 3). However, there was no recognition of an HLA-$A2^{neg}$ $pSer^{1100}$-IRS-2^+ melanoma, SK-Mel-28, or an HLA-$A2^+$, $pSer^{1100}$-IRS-2 low to negative ovarian carcinoma, OV-90. While there is no specific antibody for Ser^{42}-phosphorylated CDC25b, human CD8 T-cells transfected to express the pCDC25$b_{38\text{-}46}$-specific TCR recognized two HLA-$A2^+$ melanomas that expressed high levels of total CDC25b (MelSwift and 1102Mel), and failed to recognize either an HLA-$A2^{neg}$ CDC25b^+ melanoma, SK-Mel-28, or an HLA-$A2^+$ CDC25b^{lo} ovarian carcinoma, OV-90 (Figure 2C, 4).

We utilized these T-cells to evaluate expression of pIRS-$2_{1097\text{-}1105}$ and pCDC25$b_{38\text{-}46}$ on HLA-$A2^+$ cancer cell lines of different types. For the HLA-$A2^+$ cancer cells, we loaded the Western blots based on cell equivalents rather than protein equivalence, so we could directly compare per cell level of expression of Ser^{1100}-phosphorylated IRS-2 with T-cell recognition, which also occurs on a per cell basis. Although the amount varied, Ser^{1100}-phosphorylated IRS-2 was detected by Western blot in the majority of melanoma, ovarian cancer, colo-rectal adenocarcinoma, breast cancer, bladder cancer, and non-small cell lung cancer (NSLC) lines evaluated, but was poorly expressed in prostate cancer cells (Figure 3A, 3C). None of the bladder, prostate or NSCL cancer cells were HLA-$A2^+$ and their recognition by pIRS-$2_{1097\text{-}1105}$-specific T-cells could not be tested. However, of the HLA-$A2^+$ cell lines evaluated, pIRS-$2_{1097\text{-}1105}$ was presented by 10/10 melanomas, 3/4 ovarian carcinomas, 2/2 colorectal carcinomas, and 2/3 breast carcinomas (Figure 3B). Cancer cells that were better recognized by pIRS-$2_{1097\text{-}1105}$-specific T-cells also expressed higher amounts of $pSer^{1100}$-IRS-2 by Western blot (Figure 3D). pCDC25$b_{38\text{-}46}$-specific T-cells also did not recognize the HLA-$A2^{neg}$ cancer cells T47D and SK-Mel-28 (Figure 2C, 4B). They did recognize 3/4 HLA-$A2^+$ melanomas, 3/3 breast cancer lines (Figure 2C, 4B), and the HLA-$A2^+$ EBV-transformed lymphoblastoid cell line JY (not shown). However, although pCDC25b-specific T-cells showed high avidity and high-level recognition of peptide-pulsed targets (Figure 2B), their recognition of these cancer cells was relatively low (Figure 4B). They also did not recognize the 2 colorectal adenocarcinomas and 4 ovarian cancer cell lines evaluated. In melanoma cells, there was a direct correlation between pCDC25$b_{38\text{-}46}$-specific T-cell recognition and total CDC25b protein levels (Figure 4C). However, good pCDC25$b_{38\text{-}46}$-specific T-cell recognition was associated with high level expression of CDC25b source protein in breast, ovarian and colo-rectal cancer cells but low level expression in others. This suggests that there are differences in the level or the turnover of $pSer^{42}$-CDC25b in relation to total CDC25b protein in different histological types of cancer cells. In sum, pIRS-$2_{1097\text{-}1105}$ is endogenously processed and presented by numerous malignancies of different types, and this display elicits strong effector responses from pIRS-2-specific TCR-expressing human CD8 T-cells. In contrast, pCDC25$b_{38\text{-}46}$ is presented by melanoma, breast cancer and EBV-transformed lymphoblastoid cell lines, but its overall expression on these and other cells is more limited.

Immunohistochemical analysis of pSer^{1100}-IRS-2 expression in metastatic melanoma and normal tissues

The expression of pSer^{1100}-IRS-2 in human melanoma explants and normal tissues has not been previously evaluated. We compared sections from cell blocks containing the pSer^{1100}-IRS-2^{+} SLM2 melanoma, the pSer^{1100}-IRS-2 low to negative OV-90 ovarian carcinoma, and a melanoma metastasis to the lung, each of which had been stained in the presence or absence of blocking pIRS-2$_{1097\text{-}1105}$ phosphopeptide (Figure 5). Addition of the blocking peptide largely eliminated staining of all samples. Strong cytoplasmic staining for pSer^{1100}-IRS-2 was evident in the SLM2 melanoma, with the highest staining in cells with condensed chromosomes, undergoing mitosis (Figure 5A). Strong staining of mitotic cells was also evident in the OV-90 ovarian carcinoma, but these cells were a significantly lower fraction of the total cell number, and staining of non-mitotic cells was very weak (Figure 5B). This is consistent with the very weak pSer^{1100}-IRS-2 Western blot staining (Figure 3A) and lack of T-cell recognition by pIRS-2$_{1097\text{-}1105}$-specific T-cells (Figure 2C, 3B). Strong staining was also evident in the human melanoma lung metastasis specimen, again with the highest level in mitotic cells (Figure 5C).

We evaluated additional tissue blocks of metastatic melanoma that included adjacent “normal” parenchyma from the original invaded organ. These included heart (n=1), liver (n=1), colon (n=1), and two additional lung samples. As for Figure 5, addition of the pSer^{1100}-IRS-2 blocking peptide almost completely inhibited staining for all the samples tested (not shown). When quantified as total staining density per mm^2, the melanoma metastases varied widely in their level of anti-pSer^{1100}-IRS-2 antibody binding (Table 1). Nonetheless, strong staining densities were consistently observed in melanoma cells with mitotic figures. Weaker staining was observed in non-mitotic melanoma cells and “normal” tissue, in most cases (Figure 6 and Table 1). However, colonic epithelium showed relatively high staining densities in comparison to adjacent metastatic melanoma (Supplemental Figure 4). Colonic biopsies taken for reasons other than malignancy (and which were ultimately found to contain no histopathologic abnormalities) also showed relatively high epithelial staining densities with anti-pSer^{1100}-IRS-2 (data not shown). However, high staining densities did not extend beyond the epithelium to involve deeper portions of the colonic tissue (Supplemental Figure 4). Pulmonary epithelia also demonstrated relatively high staining densities, although these were not as high as those seen in the colonic epithelia (Table 1). These findings may relate to the normal proliferation and turnover of epithelial cells. Interestingly, peritumoral stroma (fibroblasts and blood vessels) surrounding lung metastases show increased staining relative to adjacent “normal” pulmonary parenchyma (Table 1). Overall, these data suggest that successful immunotherapy based on pSer^{1100}-IRS-2 may target dividing malignant cells, and may also target peritumoral stroma. Each of these may support tumor control (43,44). However, the data also raise the possibility that there is some risk of adverse effects on colonic and pulmonary epithelia but not other normal tissues evaluated.

Phosphopeptide-specific TCR-expressing T-cells can slow tumor outgrowth

We next determined whether these two phosphopeptides could serve as immunotherapeutic targets for treatment of cancer. NOD/SCID/IL-2Rγc$^{-/-}$ mice were inoculated

subcutaneously with SLM2 melanoma cells, and 3d later were injected with human CD8 T-cells expressing either the pIRS-2-specific or pCDC25b-specific TCR, or both populations, together with IL-2. A second infusion of transfected CD8 T-cells was given 4d later. Animals that received any of these populations remained tumor-free (tumor size less than 30 mm^2) for significantly longer than control animals that only received IL-2 (Figure 7A–C). Tumors in animals that received any of these phosphopeptide-specific murine TCR-expressing cells were significantly smaller on day 10 and 15 than those of control animals that received only IL-2 (Figure 7D). On day 18, tumors in treated animals were still smaller, but only those in mice given pCDC25b-specific T cells were still significant. No significant differences in outgrowth in any groups were evident beyond day 22, most likely due to loss of expression of phosphopeptide-specific murine TCR (Supplemental Figure 3C). Indeed, at the end of the experiment, we identified persisting human T-cells that no longer expressed murine TCR in tumor and spleens of treated animals (data not shown). Nonetheless, this demonstrates that the endogenous levels of pIRS-$2_{1097\text{-}1105}$ and pCDC25$b_{38\text{-}46}$ phosphopeptide on melanoma are sufficient for T-cell recognition and allow some control of tumor growth *in vivo*.

Discussion

In this study, we characterized two phosphopeptide TAA that are endogenously processed and presented on multiple HLA-$A2^+$ cancers. To explore the display on cancer cells, we utilized cloned murine TCR specific for each phosphopeptide and an antibody specific for the phosphorylated IRS-2 source protein. pIRS-$2_{1097\text{-}1105}$ is displayed on multiple HLA-$A2^+$ melanomas and breast, ovarian, and colo-rectal carcinomas, and this display is correlated with the level of Ser^{1100}-phosphorylated IRS-2 source protein. Mitotically active tumor cells expressed very high levels of Ser^{1100}-phosphorylated IRS-2 protein. Based on immunologically relevant levels of display of pIRS-$2_{1097\text{-}1105}$, we expect to be able to immunologically target a variety of distinct malignancies. In contrast, pCDC25$b_{38\text{-}46}$ display is restricted to melanoma and breast cancer. Although it is also displayed on lymphoblastoid cell lines, it was not found on a set of hematological malignancies (17). Nonetheless, this peptide adds to the otherwise small number of antigenic epitopes that have been defined for breast cancer.

Both phosphopeptides are strongly immunogenic *in vitro* for human T-cells and *in vivo* for HLA-A2 transgenic mice, lending credence to their utility as immunotherapeutics. Indeed, CD8 T-cell responses to these phosphopeptides in many normal healthy donors were evident primarily in the $CD45RO^+$ memory compartment. In contrast, immunological responses to cancer-testes antigens and tissue-associated differentiation antigens are usually only seen in cancer patients (45,46). Although high level responses to an HLA-A2-restricted epitope from MART-1 are seen in normal individuals, these are primarily evident in the naïve T-cell compartment (46). While it is difficult to prove in humans, we hypothesize that the memory responses to the pIRS-$2_{1097\text{-}1105}$ and pCDC25$b_{38\text{-}46}$ phosphopeptides in normal individuals are evidence of previous encounters with nascent tumors that have dysregulated phosphorylation cascades. Although we have seen expression of $pSer^{1100}$-IRS-2 protein in some normal colonic and pulmonary epithelia by immunohistochemistry, there is no evidence of autoimmunity in these healthy human donors that we have evidence of memory

phosphopeptide-specific T-cell responses. There may be self-tolerance directed against very high avidity human TCR for these antigens thus emphasizing the utility of high affinity murine TCRs for adoptive therapy.

One approach currently showing some success for the treatment of cancer patients involves the adoptive transfer of tumor-specific CD8 T-cells, generated through vaccination or by genetic modification via expression of TCR chains specific for an appropriate TAA (1). Clinical benefit following infusion of such transfected T-cells has been observed in melanoma and synovial cell sarcoma (35,39). Most of the TCR chains currently cloned and studied in human clinical trials for melanoma have been specific for melanocyte differentiation proteins (1,6,39). Although of obvious importance for melanoma, extending this form of immunotherapy to antigens that are broadly expressed on other types of cancers offers the possibility of broadening adoptive cell therapy to multiple cancer patients. In addition, we have identified phosphopeptides presented on cancer cells by other HLA alleles besides HLA-A2 (data not shown, (17)), extending the number of patients that can be treated with phosphopeptide-specific immunotherapy.

The utilization of murine TCR minimizes concerns about formation of unintended allo- or self-reactive TCRs through pairing with human endogenous TCR α and β chains while allowing isolation of chains of sufficient avidity to mediate tumor regression (37,41). We have not seen alloreaction of human cancer cells expressing other alleles than HLA-A2 when these murine TCR chains are expressed in human CD8 T-cells. While we have not directly compared the avidities of these cloned murine TCR with those of bulk short-term human CD8 T-cells, we believe that the salient issue is that the avidities of the cloned murine TCR are high and in a therapeutically useful range based on peptide dose response curves (47). Thus, we now have new tools which can be utilized to evaluate and treat cancer patients: the phosphopeptides themselves for use in active vaccination, and murine TCR chains specific for either pIRS-$2_{1097\text{-}1105}$- or pCDC25$b_{38\text{-}46}$-peptides that can be utilized as immunotherapeutic agents to re-target a patient's T cells to these post-translationally modified epitopes.

Supplementary Material

Refer to Web version on PubMed Central for supplementary material.

Acknowledgments

Financial support: Supported by USPHS Grants R01 A120963 and CA134060 (VHE), pilot project funding from the University of Virginia Cancer Center, and American Cancer Society Institutional Research Grant GF11420 (ALZ). JP was supported by USPHS Training Grant T32 AI07496 and ALZ was a recipient of a Sidney Kimmel Scholar award.

We thank all blood donors and Sara Adair for their contributions. In addition, we thank Janet Gorman and Holly Davis for maintenance of the AAD transgenic animal colony.

References

1. Rosenberg SA, Restifo NP, Yang JC, Morgan RA, Dudley ME. Adoptive cell transfer: a clinical path to effective cancer immunotherapy. Nat Rev Cancer. 2008; 8:299–308. [PubMed: 18354418]

2. Morgan RA, Dudley ME, Wunderlich JR, Hughes MS, Yang JC, Sherry RM, et al. Cancer regression in patients after transfer of genetically engineered lymphocytes. Science. 2006; 314:126–9. [PubMed: 16946036]

3. Schwartzentruber DJ, Lawson DH, Richards JM, Conry RM, Miller DM, Treisman J, et al. gp100 Peptide Vaccine and Interleukin-2 in Patients with Advanced Melanoma. New England Journal of Medicine. 2011; 364:2119–27. [PubMed: 21631324]

4. Higano CS, Schellhammer PF, Small EJ, Burch PA, Nemunaitis J, Yuh L, et al. Integrated data from 2 randomized, double-blind, placebo-controlled, phase 3 trials of active cellular immunotherapy with sipuleucel-T in advanced prostate cancer. Cancer. 2009; 115:3670–9. [PubMed: 19536890]

5. Slingluff CL, Petroni GR, Yamshchikov GV, Hibbitts S, Grosh WW, Chianese-Bullock KA, et al. Immunologic and clinical outcomes of vaccination with a multiepitope melanoma peptide vaccine plus low-dose interleukin-2 administered either concurrently or on a delayed schedule. J Clin Oncol. 2004; 22:4474–85. [PubMed: 15542798]

6. Rosenberg SA, Yang JC, Restifo NP. Cancer immunotherapy: moving beyond current vaccines. Nat Med. 2004; 10:909–15. [PubMed: 15340416]

7. Williamson NA, Rossjohn J, Purcell AW. Tumors reveal their secrets to cytotoxic T cells. Proc Natl Acad Sci U S A. 2006; 103:14649–50. [PubMed: 17005729]

8. Simpson AJ, Caballero OL, Jungbluth A, Chen YT, Old LJ. Cancer/testis antigens, gametogenesis and cancer. Nat Rev Cancer. 2005; 5:615–25. [PubMed: 16034368]

9. Hogan KT, Eisinger DP, Cupp SB, Lekstrom KJ, Deacon DD, Shabanowitz J, et al. The peptide recognized by HLA-A68.2-restricted, squamous cell carcinoma of the lung-specific cytotoxic T lymphocytes is derived from a mutated elongation factor 2 gene. Cancer Res. 1998; 58:5144–50. [PubMed: 9823325]

10. Dunn GP, Old LJ, Schreiber RD. The three Es of cancer immunoediting. Annu Rev Immunol. 2004; 22:329–60. [PubMed: 15032581]

11. Hirohashi Y, Torigoe T, Inoda S, Kobayasi J, Nakatsugawa M, Mori T, et al. The functioning antigens: beyond just as the immunological targets. Cancer Sci. 2009; 100:798–806. [PubMed: 19445013]

12. Hunter T. Signaling--2000 and beyond. Cell. 2000; 100:113–27. [PubMed: 10647936]

13. Sjoblom T, Jones S, Wood LD, Parsons DW, Lin J, Barber TD, et al. The consensus coding sequences of human breast and colorectal cancers. Science. 2006; 314:268–74. [PubMed: 16959974]

14. Zarling AL, Ficarro SB, White FM, Shabanowitz J, Hunt DF, Engelhard VH. Phosphorylated peptides are naturally processed and presented by major histocompatibility complex class I molecules in vivo. J Exp Med. 2000; 192:1755–62. [PubMed: 11120772]

15. Depontieu FR, Qian J, Zarling AL, McMiller TL, Salay TM, Norris A, et al. Identification of tumor-associated, MHC class II-restricted phosphopeptides as targets for immunotherapy. Proc Natl Acad Sci USA. 2009; 106:12073–8. [PubMed: 19581576]

16. Zarling AL, Polefrone JM, Evans AM, Mikesh LM, Shabanowitz J, Lewis ST, et al. Identification of class I MHC associated phosphopeptides as targets for cancer immunotherapy. Proc Natl Acad Sci U S A. 2006; 103:14889–94. [PubMed: 17001009]

17. Cobbold M, De La Peña H, Norris A, Polefrone JM, Qian J, English AM, et al. MHC Class I-associated phosphopeptides are the targets of memory-like immunity in leukemia. Sci Transl Med. 2013; 5:203ra125.

18. Dearth RK, Cui X, Kim HJ, Hadsell DL, Lee AV. Oncogenic Transformation by the Signaling Adaptor Proteins Insulin Receptor Substrate (IRS)-1 and IRS-2. Cell Cycle. 2007; 6:705–13. [PubMed: 17374994]

19. Kornmann M, Maruyama H, Bergmann U, Tangvoranuntakul P, Beger HG, White MF, et al. Enhanced expression of the insulin receptor substrate-2 docking protein in human pancreatic cancer. Cancer Research. 1998; 58:4250–4. [PubMed: 9766646]

20. Boissan M, Beurel E, Wendum D, Rey C, Lecluse Y, Housset C, et al. Overexpression of insulin receptor substrate-2 in human and murine hepatocellular carcinoma. Am J Pathol. 2005; 167:869–77. [PubMed: 16127164]

21. Kim B, van Golen CM, Feldman EL. Insulin-like growth factor-I signaling in human neuroblastoma cells. Oncogene. 2004; 23:130–41. [PubMed: 14712218]
22. Jackson JG, Zhang X, Yoneda T, Yee D. Regulation of breast cancer cell motility by insulin receptor substrate-2 (IRS-2) in metastatic variants of human breast cancer cell lines. Oncogene. 2001; 20:7318–25. [PubMed: 11704861]
23. Knobbe CB, Reifenberger G. Genetic alterations and aberrant expression of genes related to the phosphatidyl-inositol-3′-kinase/protein kinase B (Akt) signal transduction pathway in glioblastomas. Brain Pathol. 2003; 13:507–18. [PubMed: 14655756]
24. Parsons DW, Wang TL, Samuels Y, Bardelli A, Cummins JM, DeLong L, et al. Colorectal cancer: mutations in a signalling pathway. Nature. 2005; 436:792. [PubMed: 16094359]
25. Chan BT, Lee AV. Insulin Receptor Substrates (IRSs) and Breast Tumorigenesis. J Mammary Gland Biol Neoplasia. 2008; 13:415–22. [PubMed: 19030971]
26. Dearth RK, Cui X, Kim HJ, Kuiatse I, Lawrence NA, Zhang X, et al. Mammary tumorigenesis and metastasis caused by overexpression of insulin receptor substrate 1 (IRS-1) or IRS-2. Mol Cell Biol. 2006; 26:9302–14. [PubMed: 17030631]
27. Nagle JA, Ma Z, Byrne MA, White MF, Shaw LM. Involvement of insulin receptor substrate 2 in mammary tumor metastasis. Mol Cell Biol. 2004; 24:9726–35. [PubMed: 15509777]
28. Dephoure N, Zhou C, Villén J, Beausoleil SA, Bakalarski CE, Elledge SJ, et al. A quantitative atlas of mitotic phosphorylation. PNAS. 2008; 105:10762–7. [PubMed: 18669648]
29. Kiyokawa H, Ray D. In vivo roles of CDC25 phosphatases: biological insight into the anti-cancer therapeutic targets. Anticancer Agents Med Chem. 2008; 8:832–6. [PubMed: 19075565]
30. Lindqvist A, Kallstrom H, Karlsson Rosenthal C. Characterisation of Cdc25B localisation and nuclear export during the cell cycle and in response to stress. J Cell Sci. 2004; 117:4979–90. [PubMed: 15456846]
31. Tsai V, Kawashima I, Keogh E, Daly K, Sette A, Celis E. In vitro immunization and expansion of antigen-specific cytotoxic T lymphocytes for adoptive immunotherapy using peptide-pulsed dendritic cells. Crit Rev Immunol. 1998; 18:65–75. [PubMed: 9419449]
32. Slingluff CL, Petroni GR, Olson WC, Smolkin ME, Ross MI, Haas NB, et al. Effect of Granulocyte/Macrophage Colony-Stimulating Factor on Circulating CD8+ and CD4+ T-Cell Responses to a Multipeptide Melanoma Vaccine: Outcome of a Multicenter Randomized Trial. Clin Cancer Res. 2009; 15:7036–7044. [PubMed: 19903780]
33. Santomasso BD, Roberts WK, Thomas A, Williams T, Blachere NE, Dudley ME, et al. A T-cell receptor associated with naturally occurring human tumor immunity. Proc Natl Acad Sci U S A. 2007; 104:19073–8. [PubMed: 18045792]
34. Brochet X, Lefranc M-P, Giudicelli V. IMGT/V-QUEST: the highly customized and integrated system for IG and TR standardized V-J and V-D-J sequence analysis. Nucleic Acids Res. 2008; 36:W503–508. [PubMed: 18503082]
35. Johnson LA, Heemskerk B, Powell DJ, Cohen CJ, Morgan RA, Dudley ME, et al. Gene Transfer of Tumor-Reactive TCR Confers Both High Avidity and Tumor Reactivity to Nonreactive Peripheral Blood Mononuclear Cells and Tumor-Infiltrating Lymphocytes. J Immunol. 2006; 177:6548–59. [PubMed: 17056587]
36. Zhao Y, Zheng Z, Cohen CJ, Gattinoni L, Palmer DC, Restifo NP, et al. High-efficiency transfection of primary human and mouse T lymphocytes using RNA electroporation. Mol Ther. 2006; 13:151–9. [PubMed: 16140584]
37. Cohen CJ, Zhao Y, Zheng Z, Rosenberg SA, Morgan RA. Enhanced Antitumor Activity of Murine-Human Hybrid T-Cell Receptor (TCR) in Human Lymphocytes Is Associated with Improved Pairing and TCR/CD3 Stability. Cancer Res. 2006; 66:8878–86. [PubMed: 16951205]
38. Johnson LA, Morgan RA, Dudley ME, Cassard L, Yang JC, Hughes MS, et al. Gene therapy with human and mouse T-cell receptors mediates cancer regression and targets normal tissues expressing cognate antigen. Blood. 2009; 114:535–46. [PubMed: 19451549]
39. Park TS, Rosenberg SA, Morgan RA. Treating cancer with genetically engineered T cells. Trends Biotechnol. 2011; 29:550–7. [PubMed: 21663987]
40. Effros RB. Role of T lymphocyte replicative senescence in vaccine efficacy. Vaccine. 2007; 25:599–604. [PubMed: 17014937]

41. Stauss HJ, Cesco-Gaspere M, Thomas S, Hart DP, Xue SA, Holler A, et al. Monoclonal T-Cell Receptors: New Reagents for Cancer Therapy. Mol Ther. 2007; 15:1744–50. [PubMed: 17637721]

42. Jorritsma A, Gomez-Eerland R, Dokter M, van de Kasteele W, Zoet YM, Doxiadis I, et al. Selecting highly affine and well-expressed TCRs for gene therapy of melanoma. Blood. 2007; 110:3564–72. [PubMed: 17660381]

43. Zhang B, Bowerman NA, Salama JK, Schmidt H, Spiotto MT, Schietinger A, et al. Induced sensitization of tumor stroma leads to eradication of established cancer by T cells. J Exp Med. 2007; 204:49–55. [PubMed: 17210731]

44. Zhang B, Zhang Y, Bowerman NA, Schietinger A, Fu YX, Kranz DM, et al. Equilibrium between host and cancer caused by effector T cells killing tumor stroma. Cancer Res. 2008; 68:1563–71. [PubMed: 18316622]

45. Scanlan MJ, Gure AO, Jungbluth AA, Old LJ, Chen Y-T. Cancer/testis antigens: an expanding family of targets for cancer immunotherapy. Immunological Reviews. 2002; 188:22–32. [PubMed: 12445278]

46. Pittet MJ, Valmori D, Dunbar PR, Speiser DE, Lienard D, Lejeune F, et al. High frequencies of naive Melan-A/MART-1-specific CD8(+) T cells in a large proportion of human histocompatibility leukocyte antigen (HLA)-A2 individuals. J Exp Med. 1999; 190:705–15. [PubMed: 10477554]

47. Zhong S, Malecek K, Johnson LA, Yu Z, de Miera EV-S, Darvishian F, et al. T-cell receptor affinity and avidity defines antitumor response and autoimmunity in T-cell immunotherapy. PNAS. 2013; 110:6973–8. [PubMed: 23576742]

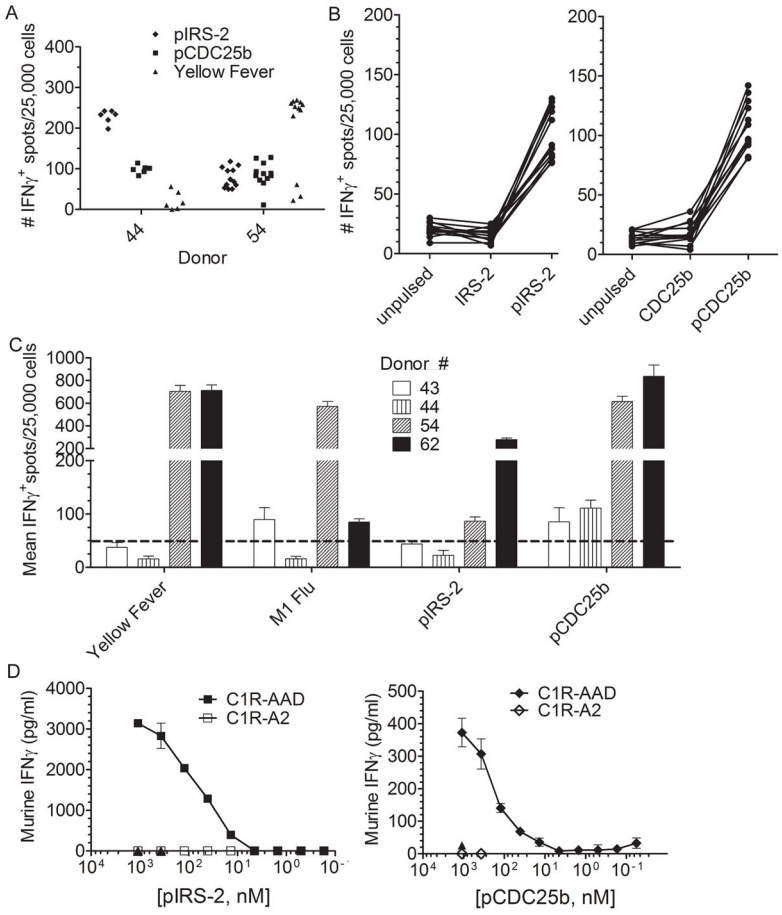

Figure 1. Phosphopeptides from IRS-2 and CDC25b are immunogenic *in vitro* for human CD8 T-cells and *in vivo* for AAD transgenic mice

Bulk (A, B) and CD45RO$^+$ memory (C) CD8 T-cells from HLA-A2$^+$ donors were restimulated *in vitro* in 6–12 replicate microcultures with pIRS-2$_{1097\text{-}1105}$, pCDC25b$_{38\text{-}46}$, M1$_{58\text{-}66}$ Flu, or Yellow Fever NS4B$_{214\text{-}222}$ peptide-pulsed DC for 7d. Antigen-specific T-cells were detected by ELIspot using T2 stimulators pulsed with the indicated peptide. “p” refers to the phosphorylated form of each peptide. (A, B) Each data point represents an individual 7d microculture. All donor responses were tested in 3 separate experiments with 1 representative experiment shown. (C) Mean # of IFN-γ$^+$ memory CD8 T-cells to the indicated peptide. Dotted line shows response cutoff of 50 spots/25,000 cells. (D) IFN-γ production by murine CD8 T-cell lines specific for the indicated phosphopeptide following co-culture with C1R-AAD or C1R-A2 targets pulsed with either pIRS-2$_{1097\text{-}1105}$ (left) or pCDC25b$_{38\text{-}46}$ (right) for 24h. C1R-AAD targets pulsed with unphosphorylated peptides are indicated with triangles. Data representative of 3–4 separate experiments.

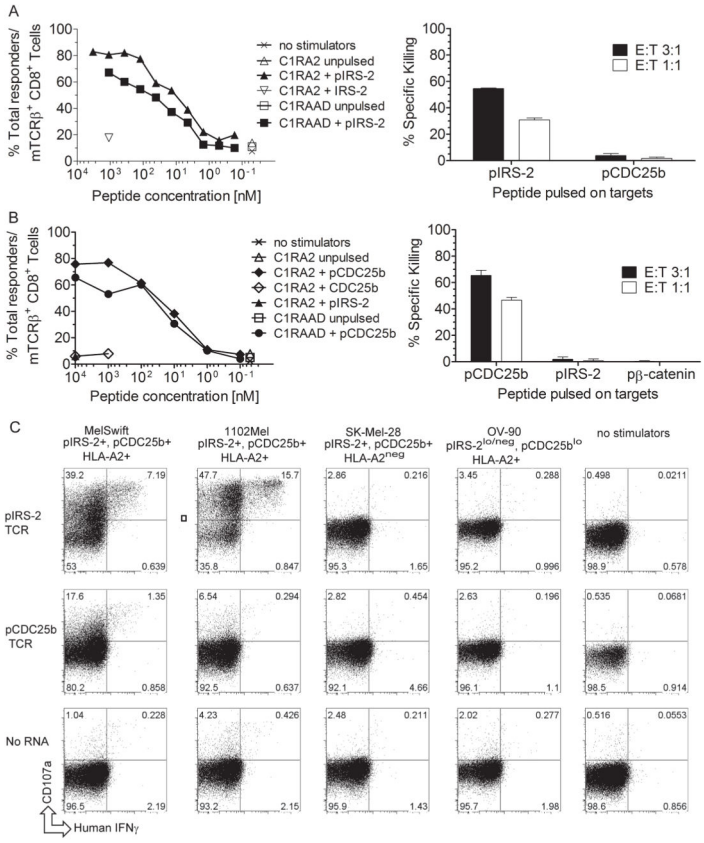

Figure 2. Expression of phosphopeptide-specific murine TCR in human CD8 T-cells confers recognition of HLA-A2$^+$ targets and effector function

Human CD8 T-cells were electroporated with IVT RNA encoding phosphopeptide-specific murine TCR αβ chains, and assayed 12–14h later. (A, B) *left panels*, pIRS-2-specific (A) or pCDC25b-specific (B) human CD8 T-cells were co-cultured with the indicated targets for 5hrs and the percentage mTCRβ$^+$ human CD8$^+$ cells expressing surface either CD107a or intracellular IFN-γ or both (total responders) detected by flow cytometry. *Right panels*, pIRS-2-specific (A) or pCDC25b-specific (B) CD8 T-cells were cultured with phosphopeptide-pulsed (CFSE^{hi}) or unpulsed (CFSE^{lo}) C1R-A2 targets, and specific cytotoxic activity was evaluated. (C) pIRS-2-specific or pCDC25b-specific human CD8 T-cells were co-cultured with the indicated human cancer cells and surface CD107a and/or intracellular IFN-γ on gated mTCRβ$^+$ cells were detected by flow cytometry. Antigen expression was determined by Western blot and is shown in Figures 3 and 4. For all panels, data are representative of duplicate (triplicate for *in vitro* cytotoxicity assay) determinations in 2–5 experiments.

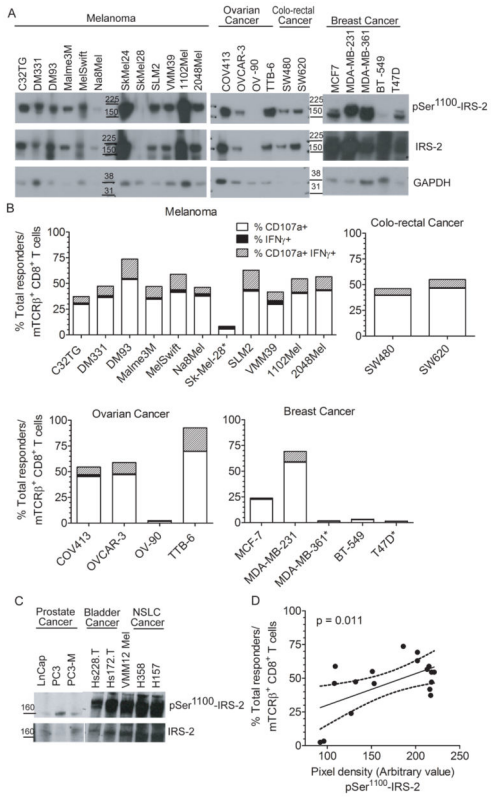

Figure 3. pIRS-2$_{1097\text{-}1105}$ is endogenously processed and presented by cancer cells of multiple histological types

(A) Immunoblots showing expression of pSer^{1100}-IRS-2 (*top*), total IRS-2 (*middle*) and GAPDH (*bottom*) in extracts representing 1.5×10^5 cell equivalents of the indicated cell lines. Anti-pSer^{1100}-IRS-2 and anti-GAPDH staining was done simultaneously for each blot, which was then stripped and reprobed with anti-IRS-2 (5 min exposure for all blots). Because lysates were loaded based on equivalent cell numbers instead of protein, the evident variation in GAPDH protein indicates differences in expression of this housekeeping gene in different cancer cells. Data are from a single experiment representative of 4. (B) Total responding pIRS-2-specific human CD8 T-cells (mTCRβ$^+$ human CD8$^+$) following co-culture with indicated human cancer cells was determined as in Figure 2. HLA-A2-negative cancer cell lines are indicated with a *. Data is representative of 3–5 experiments. (C) Immunoblots of pSer^{1100}-IRS-2 (*top*) and total IRS-2 (*bottom*) in extracts representing 50 μg total protein of the indicated cancer cells. (D) Correlation between pSer^{1100}-IRS-2 protein and recognition of HLA-A2$^+$ cancer cells by pIRS-2-specific mTCRβ$^+$ human CD8 T-cells (data in A & B). Linear regression analysis (solid line) with 95% confidence intervals (dashed lines) is shown. P value indicates Best-Fit value for the slope of the curve being significantly non-zero.

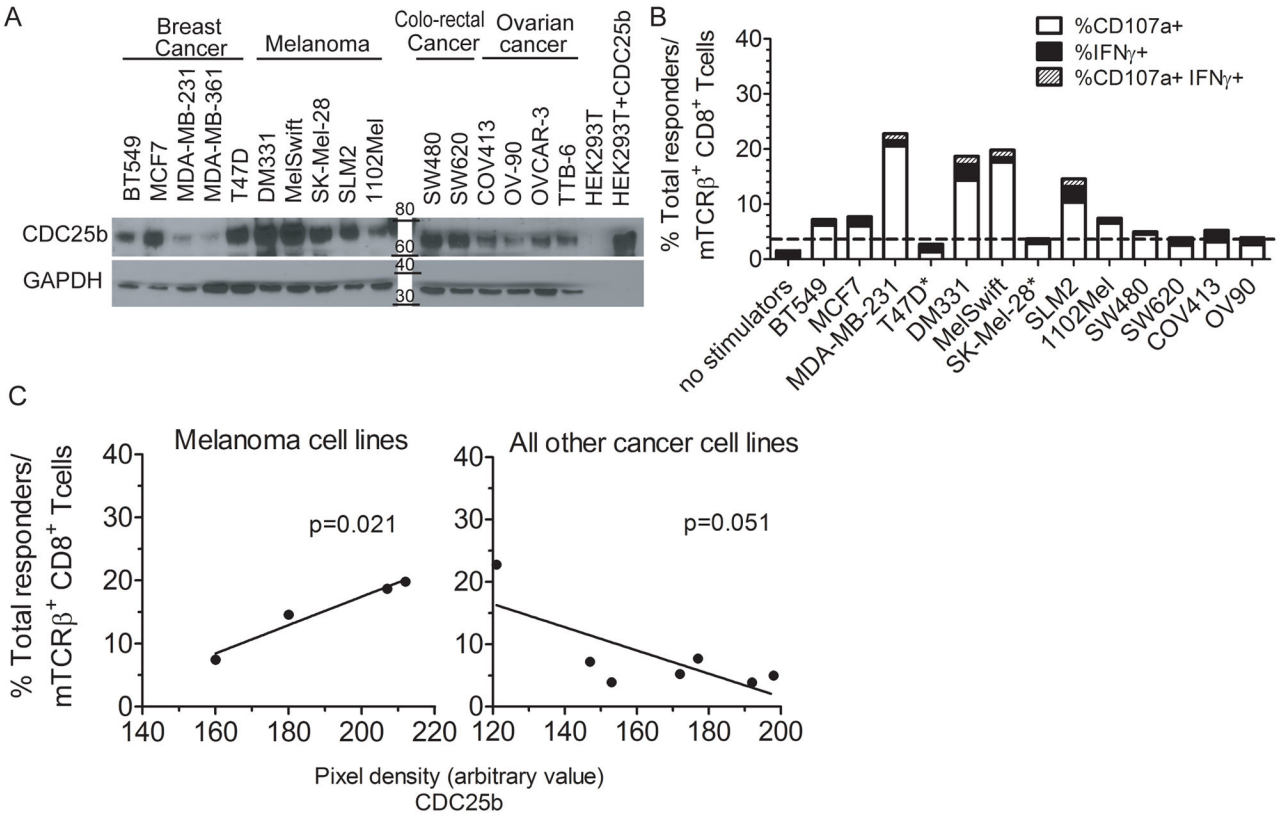

Figure 4. pCDC25b$_{38-46}$-specific TCR-expressing human CD8 T-cells recognize endogenously processed and presented phosphopeptide on human melanoma and breast cancer cells

(A) Immunoblots showing expression of total CDC25b (*top*) and GAPDH (*bottom*) in indicated cancer cells (30 μg cytoplasmic protein). Only 1μg of a CDC25b-transfected HEK293T cell lysate was loaded in order to not over-expose blot, resulting in an almost undetectable GAPDH signal. Representative blots from 2 experiments shown. (B) Total responding pCDC25b-specific human CD8 T-cells (mTCRβ$^+$ human CD8$^+$) following co-culture with indicated human cancer cells was determined as described in Figure 2. HLA-A2-negative cancer cells are indicated with a * and dashed line indicates background following co-culture with these HLA-A2^{neg} cancer cells. Data representative of 2 experiments. (C) Correlation between CDC25b protein level and recognition of HLA-A2$^+$ cancer cells by pCDC25b-specific mTCRβ$^+$ human CD8 T-cells in melanoma cell lines, *left panel*, and all other cancer cell lines evaluated, *right panel* (data in A & B). Analysis completed as in Figure 3D.

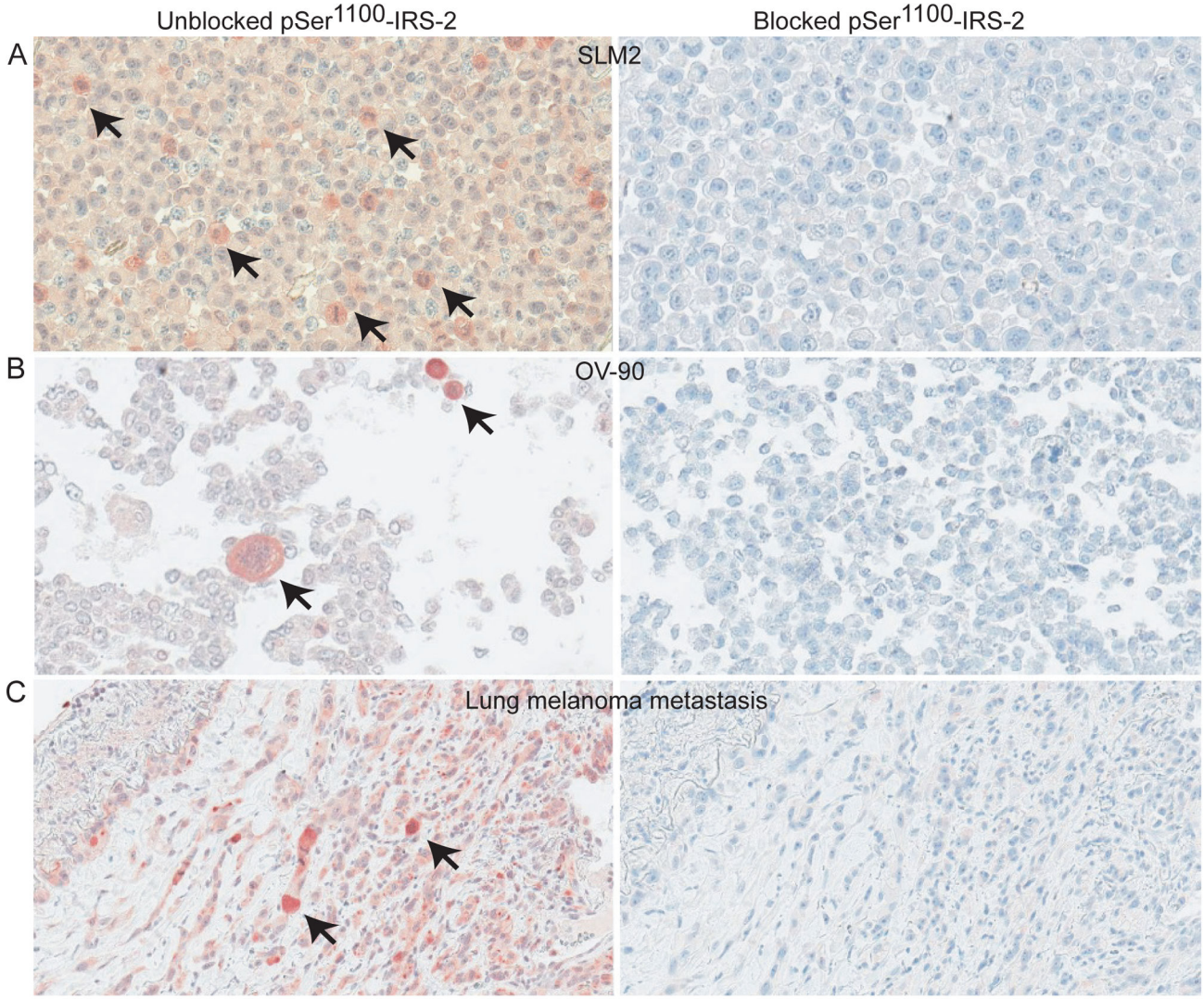

Figure 5. pSer^{1100}-IRS-2 staining is highest in mitotic cancer cells

pSer^{1100}-IRS-2 stained tissue sections from the melanoma cell line SLM2 (A), ovarian carcinoma OV-90 (B), and lung melanoma metastasis 1 (see Table 1) (C) without (*left*) or with (*right*) blocking peptide added to antibody prior to staining. All images are 100X magnification. Arrows indicate mitotic cells.

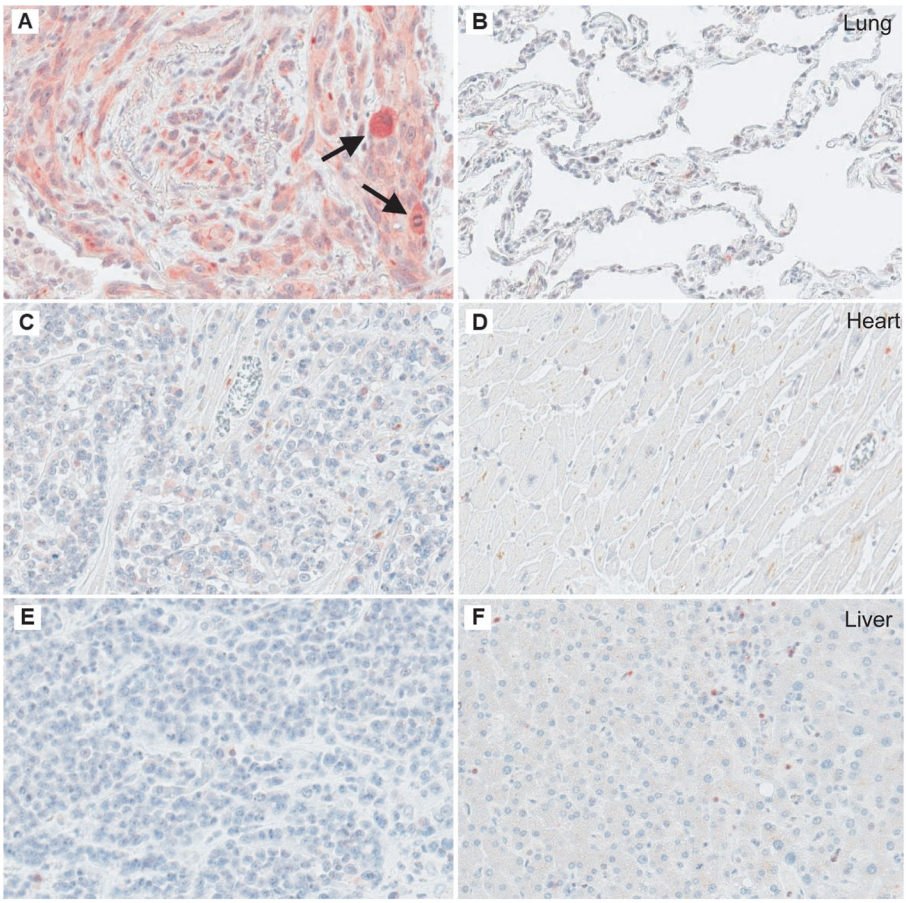

Figure 6. Ser^{1100}-phosphorylated IRS-2 expression in metastatic melanoma sections involving vital organs

pSer^{1100}-IRS-2 stained sections from melanoma metastases in lung (sample 3 in Table 1), heart and liver (A, C and E, respectively), together with adjacent uninvolved tissues (B, D, and F, respectively). Arrows in A indicate mitotic cells with intense staining. All images are 100X magnification.

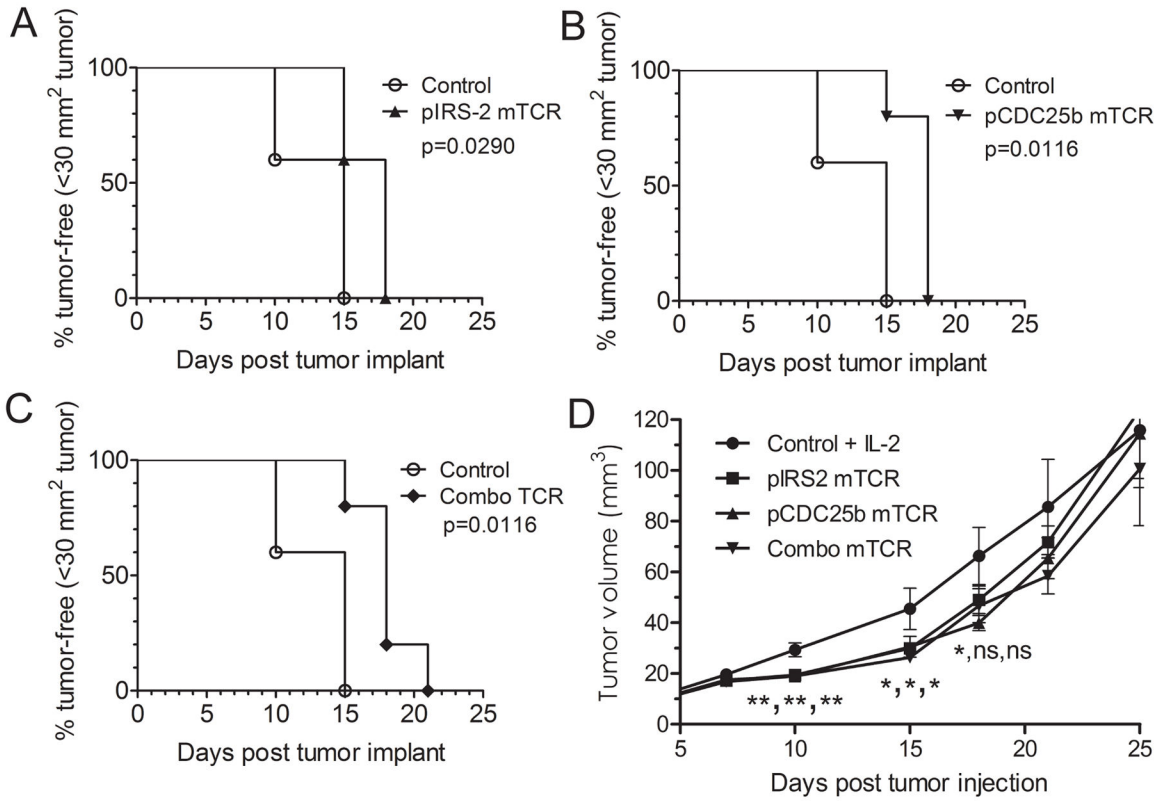

Figure 7. Enhanced tumor-free survival and delayed tumor outgrowth following adoptive transfer of phosphopeptide-specific TCR-expressing human CD8 T-cells

SLM2AAD melanoma tumor-bearing NOD/SCID/IL-2Rγc$^{-/-}$ mice were injected with phosphopeptide-specific TCR-expressing human CD8 T-cells on days 3 and 7, together with 1500 CU/ml IL-2 every other day for 10 days. Control animals received only IL-2. Combo TCR animals received equal amounts of pIRS-2 and pCDC25b-TCR expressing human CD8 T-cells. (n= 5 per group). (A–C) P values were determined by Log-rank (Mantel Cox Test) analysis of control animals to the indicated experimental group through day 25. (D) Data points are mean tumor volumes for each group +/− SD. P values were determined by ANOVA with post-hoc comparisons and no adjustment for multiple comparisons for each day and are in the sequence pCDC25b-TCR, pIRS2, and combo TCR. **, p=0.004, *, p=0.025, ns, p>0.05.

Table 1

Specific anti-Ser^{1100}-pIRS-2 staining densities (positive pixel count x $10^7/mm^2$) for melanoma metastases and surrounding tissues

Tissue specimen	Melanoma metastasis	Adjacent "normal" tissue	Pseudostratified respiratory epithelium within normal tissue	Peritumoral stroma
Heart muscle with melanoma metastasis	2.2	0.4	ND	ND
Liver with melanoma metastasis	1.5	4.3	ND	ND
Lung with melanoma metastasis 1	7.1	9.8	21	14
Lung with melanoma metastasis 2	6.1	1.7	5.5	2.8
Lung with melanoma metastasis 3	9.4	2.5	ND	ND
Colon with melanoma metastasis	3.3	1.6 –34	ND	ND
Mean in mitotic cells (lung with melanoma metastasis 2)**	27	ND	ND	ND
Mean in mitotic cells (SLM2 melanoma)*	419.5	ND	ND	ND

Specific staining densities were calculated as described in Methods. ND = not done.

** mean for mitotic cells (n=5) in Lung melanoma metastasis 1 (Figure 5C).

* mean for mitotic cells (n=5) in SLM2 melanoma cells *in vitro*.